ELSEVIER

Chemical Engineering Journal 69 (1998) 27–38

Chemical Engineering Journal

Design and operational performance of conveyor-belt drying structures

C.T. Kiranoudis *

Department of Chemical Engineering, National Technical University, GR-15780, Athens, Greece

Received 14 April 1997; revised 22 August 1997; accepted 24 September 1997

Abstract

The design and operational characteristics of conveyor-belt dryers constitute an important field of chemical engineering, which is still governed by empiricism. In this work, both aspects were studied in a straightforward way based on mathematical reasoning. A mathematical model describing the convective drying process was developed. Design procedures aimed at the determination of optimum equipment arrangement, size and operational characteristics for conveyor-belt dryers were carried out by optimizing the total annual cost of each equipment arrangement for a given production capacity. All dryer arrangements were compared by evaluating optimum configurations for a wide range of production capacity values. Once the dryer configuration was specified, its operational performance was evaluated by comparing the optimum operational cost versus production capacity for a specific optimum designed structure. An example covering the drying of sliced potato is included to demonstrate the performance of each design case, as well as the effectiveness of the proposed approach. © 1998 Elsevier Science S.A.

Keywords: Conveyor-belt; Convective drying process; Operational performance; Design

1. Introduction

Process design is principally a combination of configuration and parametric optimization efforts, carried out under certain flowsheet constraints available for the various stages of processing. In the case of dryers, design has become an increasingly challenging problem aimed at the evaluation of the proper type of equipment, its associated flowsheet arrangement, the optimum construction characteristics, and the operating conditions of each unit involved in the overall design. In addition, auxiliary equipment should be appropriately chosen together with their performance characteristics. However, most design efforts in this field face problems of extreme difficulty related to complex drying conditions that include many interconnected and opposing phenomena, chiefly in relation to the complex nature of drying [1]. In addition, although numerous theories have been developed for modeling drying processes, the thermophysical properties and transport coefficients that most models incorporate are in the majority of cases only imprecisely known, producing inaccurate or erroneous results on large-scale industrial applications.

Comparative design of dryers is the only way to quantify the rival solutions for use in decision-making strategies. In this procedure, determination of the appropriate dryer arrangement and its corresponding operational characteristics are considered to be a complex problem. This is usually tackled by means of empirical or semi-empirical methods [2–4]. Thygeson and Grossmann [5] presented a mathematical model for the modeling and optimization of a through-circulation packed bed dryer. Brook and Bakker-Arkema [6] determined the optimum operational parameters and size of two-stage and three-stage concurrent-flow grain dryers with intermediate tempering stages. The objective function was based on energy and capital costs. The operational parameters were constrained by the desired final moisture content and the maximum allowable value of important grain quality factors. Becker et al. [7] used a simple process model applicable for microcomputer-based on-line applications, to optimize the operation of a multi-stage grain dryer. Bertin and Blazquez [8] presented a mathematical model for a tunnel-dehydrator of the California type for plum drying, and optimized the production rate of the dryer. Kaminski et al. [9] used two methods of multi-objective optimization in order to analyse the process conditions of L-lysine drying in a fluidised bed dryer. Results obtained were compared to those of one-objective optimization. Chen [10] developed a mathematical model based on liquid diffusion theory and basic heat and mass transfer principles in order to simulate and optimize a two-stage drying system, which involved a

* Corresponding author.

PII S1385-8947(97)00102-2

fluidized and a fixed bed dryer. Vagenas and Marinos-Kouris [11] presented a mathematical model for the design and optimization of an industrial dryer for Sultana grapes. The optimal conditions were evaluated by minimizing the thermal load of the dryer per unit mass of dry product. Kiranoudis et al. [12] developed a mathematical model suitable for the design and optimization of conveyor-belt dryers. The objective of design was the evaluation of optimum flowsheet structure, construction characteristics, and operational conditions. The methodology adopted was based on constructing a superstructure involving a large number of minor structures, and optimizing it by means of non-linear mathematical programming techniques. The methodology was further expanded to include production planning analysis of multiproduct dehydrated plants [13] and flexible design under production planning criteria for conveyor-belt dryers [14,15]. Transferring mathematical programming analysis involving superstructure techniques to this area of dryer design needs further investigation. The remaining issues to be handled concern sensitivity analysis with respect to process variables having importance for the performance of the dryer as well as consideration of the actual operational performance under variable production conditions.

This present work addresses important design and operational aspects of conveyor-belt industrial dryer arrangements in detail. The process was described by developing a mathematical model. The structure, sizing and operational characteristics for a certain level of production capacity were evaluated by optimizing the total annual cost resulting from the construction and operation of a new plant. Optimum configurations were evaluated for a wide range of production capacities, comparing all configurations during the last stages of a selection procedure. The operational performance of all configurations was evaluated by comparing the optimum operational cost versus production capacity for predefined optimum designed configurations, thus comparing in a straightforward way design versus operation.

2. Mathematical modeling of conveyor-belt dryers

An industrial conveyor-belt dryer typically consists of drying chambers placed in series. Best performance is achieved when these elementary modules are grouped together into drying sections. All chambers in a drying section are equipped with a common conveyor-belt, on which the product to be dried is uniformly distributed at the entrance. Redistribution of the product takes place when it leaves a drying section and enters the one that follows. Each drying chamber is equipped with an individual heating utility and fans for air circulation through the product. Steam-operated heat exchangers are typically used for heating air, that on entering the chamber is mixed with the recirculation at a point below the heat exchange units. The construction of conveyor-belt dryers does not allow direct heating of the product by means of combustion of waste gases, thus drying medium temperatures

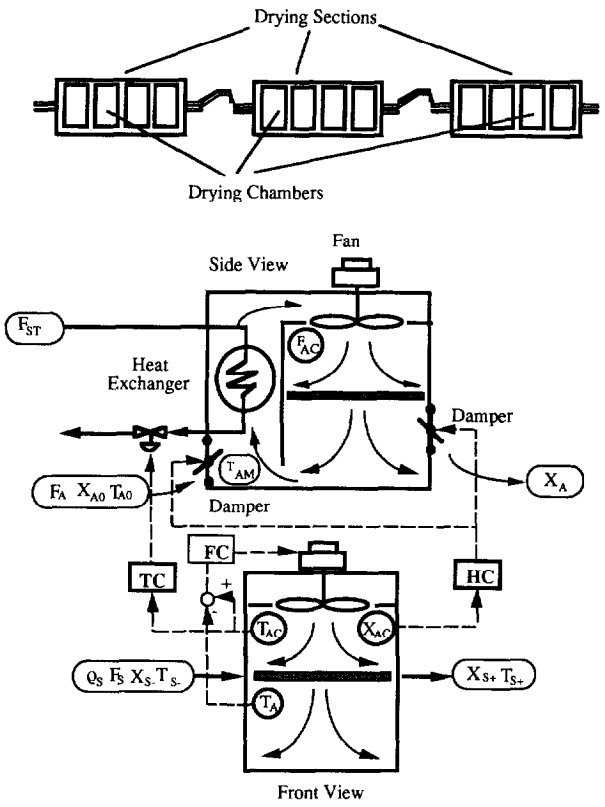

Fig. 1. Flowsheet of conveyor-belt dryer involving sections and chambers.

are confined from low to moderate levels. It is common practice that within each chamber, temperature and humidity of the air drying stream as well as its temperature diminution through the conveyor-belt, are controlled. In this case, the final control elements are the steam valve, the chamber dampers and the flow rate through the fans flowrate, which regulate the exchanged heat rate at heat exchangers, the flow rate of air streams within the drying chamber and the drying rate respectively. A typical flowsheet with a sketch of the interior of a drying chamber, as well as the arrangement of its overall control facilities, is presented in Fig. 1.

Assuming that a typical conveyor-belt dryer consists of M drying sections, and that its mth section ($m=1,\ldots,M$) comprises n chambers ($n=1,\ldots,n_m$) the mathematical model describing the drying process for each individual drying chamber can be evaluated. Since each dryer is made up of similar modules, the overall steady-state mathematical model will be formed by repetition of the individual modules. The mathematical model of each drying chamber module involves heat and mass transfer balances of air and product streams, as well as heat and mass transfer phenomena that take place during drying. The system of equations generated, is subject to product quality, equipment construction, and process thermodynamic constraints, which must also be taken into consideration.

The overall steady-state mathematical model for each dryer is presented in Table 1. Eqs. (1) and (2) express the humidity balance in the drying chamber and its compartment, respectively, while Eqs. (3) and (4) state the corresponding heat

Table 1
Mathematical model of conveyor-belt dryers

$$F_{AC}^{m,n}(X_A^{m,n}-X_{AC}^{m,n})=F_A^{m,n}(X_A^{m,n}-X_{A0}) \quad (1)$$

$$F_A^{m,n}(X_A^{m,n}-X_{A0})=F_S(X_{S-}^{m,n}-X_{S+}^{m,n}) \quad (2)$$

$$Q^{m,n}-F_A^{m,n}[h_A(T_A^{m,n},X_A^{m,n})-h_A(T_{A0},X_{A0})]=F_{AC}^{m,n}[h_A(T_{AC}^{m,n},X_{AC}^{m,n})-h_A(T_A^{m,n},X_A^{m,n})] \quad (3)$$

$$F_{AC}^{m,n}[h_A(T_{AC}^{m,n},X_{AC}^{m,n})-h_A(T_A^{m,n},X_A^{m,n})]=F_S[h_S(T_{S+}^{m,n},X_{S+}^{m,n})-h_S(T_{S-}^{m,n},X_{S-}^{m,n})] \quad (4)$$

$$X_{S+}^{m,n}=X_{SE}(T_{AC}^{m,n},a_{WC}^{m,n})+[X_{S-}^{m,n}+X_{SE}(T_{AC}^{m,n},a_{WC}^{m,n})]\exp[-k_M(T_{AC}^{m,n},X_{AC}^{m,n},V_A^{m,n},d_p)t^{m,n}] \quad (5)$$

$$T_{S+}^{m,n}=T_A^{m,n} \quad (6)$$

$$a_{WC}^{m,n}=\frac{X_{AC}^{m,n}P}{(\lambda_B+X_{AC}^{m,n})P^{sat}(T_{AC}^{m,n})} \quad (7)$$

$$\rho_B^{m,n}=\frac{F_S(1+X_{S-}^{m,n})t^{m,n}}{A^{m,n}} \quad (8)$$

$$V_A^{m,n}=\frac{F_{AC}^{m,n}(1+X_{AC}^{m,n})}{A^{m,n}\rho_A} \quad (9)$$

$$Q^{m,n}=F_{ST}\Delta H^{vap}(T_{ST}) \quad (10)$$

$$Q^{m,n}=A_{ST}^{m,n}U_{ST}[(T_{ST}-T_{AM}^{m,n})-(T_{ST}-T_{AC}^{m,n})]/\ln\frac{(T_{ST}-T_{AM}^{m,n})}{(T_{ST}-T_{AC}^{m,n})} \quad (11)$$

$$F_{AC}^{m,n}h_A(T_{AM}^{m,n},X_{AC}^{m,n})=F_A^{m,n}h_A(T_{A0},X_{A0})+(F_{AC}^{m,n}-F_A^{m,n})h_A(T_A^{m,n},X_A^{m,n}) \quad (12)$$

$$\Delta T^{m,n}=T_{AC}^{m,n}-T_A^{m,n} \quad (13)$$

$$E^{m,n}=\Delta PF_{AC}^{m,n} \quad (14)$$

$$X_{S-}^{m,n}=X_{S+}^{m,n+1} \quad (15)$$

$$T_{S-}^{m,n}=T_{S+}^{m,n+1} \quad (16)$$

$$X_{S-}^{1,1}=X_{SI} \quad (17)$$

$$X_{S+}^{M,nM}=X_{SF} \quad (18)$$

$$T_{SF}=T_{S+}^{M,nM} \quad (19)$$

$$\rho_B^{m,n}=\rho_{B0}\frac{1+X_{S-}^{m,n}}{1+X_{S-}^{m,1}} \quad (20)$$

$$0\le\Delta T^{m,n}\le\Delta T_{MAX} \quad (21)$$

$$T_{A0}\le T_{S+}^{m,n}\le T_{S,MAX} \quad (22)$$

$$X_{S+}^{m,n}\ge X_{SE}(T_A^{m,n},a_W^{m,n}),a_W^{m,n}=\frac{X_A^{m,n}P}{(\lambda_B+X_A^{m,n})P^{sat}(T_A^{m,n})} \quad (23)$$

$$A^{m,n}\le A_{MAX} \quad (24)$$

balance assuming negligible heat losses. Heat and mass transfer phenomena during drying are very complicated and their solution demands considerable computational time. They involve coupled transfer mechanisms both within the solid

and the gas phase. In this case, a simplified model is considered. This version has an exponential form and contains a phenomenological mass transfer coefficient, termed the drying constant. This drying constant chiefly accounts for mass diffusion within the solid phase, but also embodies boundary layer phenomena when it is considered to be a function of all process variables affecting drying. Ample accuracy is combined with sufficiently low computation time [16].

With these assumptions, mass transfer is expressed by Eq. (5). Heat transfer is chiefly controlled by the heat transfer coefficient at the air boundary layer. For the purpose of developing the particular mathematical model, it is assumed that the heat transfer coefficient takes a value high enough to allow the product stream leaving the chamber to be in thermal equilibrium with the air stream leaving the product. This assumption removes the need for an unnecessary differential equation which would not improve the model greatly.

On the basis of the above, heat transfer within the chamber is expressed by means of Eq. (6). The air water activity involved in Eq. (5), is calculated by the basic equation of a psychometric model (Eq. (7)). The distribution of the product on the conveyor-belt is characterized by the belt load variable. This variable is expressed in units of mass of product placed on the belt per unit of area, and varies with position on the belt. Its value at the entrance of each drying chamber can be calculated by means of Eq. (8). The velocity of the drying air stream passing through the solid particles is given by Eq. (9). Heat balances at the heat exchanger section of the chamber, are given by Eqs. (10) and (11). The temperature of the mixed recirculation and fresh air streams can be calculated by means of the enthalpy balance expressed by Eq. (12). The temperature diminution of the drying air stream in passing through the solid particles is given by Eq. (13), while the electrical power consumed by the operation of the fans is expressed by Eq. (14). Connection between chambers in a section and between sections in a dryer is modeled by introducing Eqs. (15) and (16). In addition to them, nominal values can be specified for each product processed in the plant, as far as its initial and desired material moisture content as well as ultimate product temperature value are concerned. This is suggested by Eqs. (17)–(19). Furthermore, Eq. (20) represents continuity for the material placed on the conveyor-belt of each chamber in a section, since it guarantees the same value for conveyor-belt velocity for all chambers in the section. It is typical that the conveyor-belt load at the entrance of each drying section takes a predefined value, common for all sections participating in the plant, corresponding to a maximum load that the conveyor belt can handle. The temperature diminution of the drying air stream on passing through the product, should not exceed a maximum value that would guarantee uniform drying, because it prevents creation of axial mass and temperature gradients within the solid particles. This is expressed by the inequality Eq. (21). In order to prevent thermal degradation of the product, its temperature should not exceed an upper limit which definitely affects its quality. This additional constraint is given by relation Eq. (22). Furthermore, thermodynamics dictate that the material moisture content of the product stream on leaving the chamber should be greater than the corresponding moisture content at equilibrium imposed by the air operating conditions in that chamber, as proposed by constraint Eq. (23). Finally, construction of the equipment requires that the area of the conveyor belt can not exceed a minimum value, as suggested by constraint Eq. (24).

The economic evaluation of the dryer is based on the determination of its total annual cost. The corresponding capital cost is affected by each chamber area (i.e., construction expenses), the area of heat exchangers and the installed power of the fans involved. Furthermore, the capital cost is affected by the cost of the conveyor-belt, which is determined by its corresponding total area within each drying section. All capital cost components obey economy of scale laws, i.e., increase in the unit size with respect to its characteristic dimensions will contribute reduced additional capital cost, per unit of size:

$$C_{CP}=\sum_{m=1}^{M}\left[\alpha_{SC}\left(\sum_{n=1}^{n_m}\right)^{n_{SC}}+\sum_{n=1}^{n_m}\left(\alpha_{D}A^{m,n_{D}}+\alpha_{F}E^{m,n_{F}}+\alpha_{ST}A_{ST}^{m,n_{ST}}\right)\right] \quad (25)$$

The operational cost of the plant involves thermal and electrical energy, consumed at heat exchangers and fans, respectively:

$$C_{OP}=\sum_{m=1}^{M}\sum_{n=1}^{n_m}\left(C_{E}E^{m,n}+C_{ST}F_{ST}^{m,n}\right) \quad (26)$$

On the basis of the above, the total annual cost of the plant can be expressed by means of the following equation:

$$C_{T}=eC_{CP}+t_{OP}C_{OP} \quad (27)$$

Given a configuration for a conveyor-belt dryer, the design variables determining the total cost, belong to a set of the form $\{T_{AC}^{m,n}, X_{AC}^{m,n}, \Delta T^{m,n}, A^{m,n} m=1,\ldots,M, n=1,\ldots,n_M\}$. These variables can represent the process in a more straightforward way, due to their explicit physical meaning, and all other variables involved in the overall process model can be calculated accordingly. When the construction and structure dependent variables are given (dryer configuration and corresponding chamber areas), the operational performance of the dryer is evaluated by utilizing the remaining process variables (temperatures, humidities and temperature diminution through the product).

The properties and transfer coefficients involved in the mathematical model of conveyor-belt dryers listed in Table 1, are generally considered to be functions of the process variables as listed separately in Table 2. Specific enthalpies of product and air streams are taken as linear functions of temperature and material moisture content, since corresponding specific heats of solid particles, dry air, water, and vapour are assumed to be constant within the desired temperature range, and can be calculated by means of Eqs. (28) and (29). Equilibrium of water between solid and gas phase is described

Table 2
Thermophysical properties and transport phenomena constants

Specific enthalpy [18]

$$h_S(X,T) = C_{PS}T + XC_{PW}T \quad (28)$$

$$h_A(X,T) = C_{PA}T + X(\Delta H_0 + C_{PV}T) \quad (29)$$

Equilibrium material moisture content [16]

$$X_{SE}(T,a_W) = \frac{X_M C(T) K(T) a_W}{[1-K(T)a_W][1-(1-C(T)a_W]} \quad (30)$$

$$C(T) = C_0 \exp(\Delta H_C / RT) \quad (31)$$

$$K(T) = K_0 \exp(\Delta H_K / RT) \quad (32)$$

Drying constant [19]

$$k_M(T,X,V,d_P) = k_0 T^{k_1} X^{k_2} V^{k_3} d_P^{k_4} \quad (33)$$

Water vapor pressure

$$P^{sat}(T) = \exp\left(A_1 - \frac{A_2}{A_3 + T}\right) \quad (34)$$

Water latent heat of vaporization

$$\Delta H^{vap}(T) = -R\frac{d[\ln P^{sat}(T)]}{d(1/T)} \quad (35)$$

by the process desorption isotherms, which can be modeled by means of the theoretically determined GAB (Guggenheim–Anderson–de Boer) equation, which sufficiently describes the equilibrium data for a wide range of products used in the dehydration process. It is described by Eq. (30). Eqs. (31) and (32) give the temperature effect described by GAB equation. The drying constant as a function of temperature, absolute humidity and velocity of the drying air stream, as well as the characteristic dimension of material particles, is given by the empirical Eq. (33). Water vapour pressure can be calculated by means of the empirical Antoine Eq. (34), over the temperature range examined. The latent heat of vaporization of water is given by the Clausius–Clapeyron Eq. (35), which makes use of the previous vapour pressure equation.

3. Application to design and operation of conveyor-belt dryers

On the basis of the above, a design strategy for any dryer type can be postulated. Given a specified product with a predefined flowrate, to be dried from an initial to a desired moisture content level, under constraints imposed by thermodynamics, construction and product quality reasoning, the following must be determined:

1. The optimum configuration when this is not clear-cut, i.e. for conveyor-belt dryers the number of drying sections as well as the number of chambers per section (flowsheet structure).
2. The appropriate sizing of the equipment (construction characteristics).
3. The best set points of controllers (operating conditions).

For the operational analysis of the process, the structure and sizing characteristics of the equipment are predefined. In this case, we seek the economic performance of a specified dryer when it is operated under different conditions, i.e., various production capacities, flexibility with respect to input variables, etc. In this way, design versus operational performance is studied and various dryer configurations can be compared in detail for selection purposes.

4. Case studies

The proposed methodology was applied to the design of a dehydration plant which treats 300 t/y db of potato, on a 2000 h/y basis (i.e., 150 kg/h db). The raw material of bulk density 1400 kg/m^3, is to be dried in the form of cubes cut in 10 mm size, with initial material moisture content level of 5 kg/kg db. The desired dried product material moisture content is 0.05 kg/kg db. Fresh air is available with a moisture content at 0.01 kg/kg db and 25°C cold conditions. The product should not be heated to temperature levels exceeding 75°C, in order to guarantee satisfactory quality. Uniform drying is achieved by not allowing drying air temperature diminution through product to exceed a value of 10°C. We seek to design all possible conveyor-belt dryer configurations that could be utilized. The maximum constructed chamber area for a conveyor-belt dryer is 5 m^2, but a 10 m^2 case can also be taken into consideration. The maximum belt load allowed by construction specifications is 50 kg/m^2 wb. The cost of a conveyor-belt chamber is K\$1.6/m^2 increased with a power law of 0.75 as area varies. Each section contributes an additional cost of K\$1.4/m^2, with a corresponding 0.3 power law for section area considered. Heat exchangers and fans add a capital cost of \$480/m^2 and \$500/kWh, increased by 0.7 and 0.3 laws respectively. Heat exchangers used are of the plate type for heating air. The unit cost of steam (120°C) is 0.16 c/kg, while electrical energy costs 8 c/kWh. The capital cost will be paid off within a period of 5 years. Economic figures refer to the Greek market for the year 1997.

Taking into consideration that the conveyor-belt dryer MINLP (Mixed Integer Non Linear Programming) case involves a great number of design variables (i.e., integer and continuous), it is definitely a cumbersome synthesis case to solve. To tackle this problem, a superstructure of drying sections comprising serial structures of chambers is postulated, and the resulting set of optimum decision variables is determined as the solution of the corresponding NLP problem, solved by means of mathematical programming techniques [15]. The superstructure will normally contain a sufficiently large number of drying sections, each one involving a reasonable number of drying chambers. Since material moisture content at the entrance and at the exit of each drying chamber is treated as design variables of the problem, the optimal solution will contain both valid and non-valid section and

chamber units, in the sense that for the non-valid units the material moisture content of the product stream entering the unit is equal to the one of the product stream leaving it, resulting in this way in a degenerate flowsheet containing the best structure. Clearly, non-valid units will not contribute to the total annual cost of the dryer, while for valid units, the optimum decision variables (i.e., construction characteristics and operating conditions) will be determined. The superstructure approach is generally considered to be a very viable method [17]. The algorithm performing the optimization may converge only to a local optimum. In this case, it would be necessary to use different starting points in order to ensure that a global optimum has been attained by the superstructure. Furthermore, it is possible that multiple optimum or near-optimum solutions are found. This is partly due to the superstructure, but mostly due to the nature of the physical phenomena taking place during drying, and to the economic parameters of the process. Multiple solutions, however, are often desirable since one may prefer one configuration over another, if it is less difficult to construct or operate.

The postulated superstructure involved a total number of 10 drying sections, each one consisting of 15 drying chambers (i.e., 150 drying chambers in total). The total number of design variables was 599 ($150\times4-1$), including humidity and temperature of drying air and temperature diminution in each chamber and material moisture content between chambers (initial and desired values are given). Nonlinear constrained optimization throughout this paper, was carried out by means of the successive quadratic programming algorithm in the form of subroutine E04UCF/NAG. The overall mathematical model of the dryer was solved sequentially for each module involved. The code was executed on a SG Indy workstation under Unix.

5. Results and discussion

The result of the superstructure optimization for a 5 m^2 maximum allowable chamber area constraint was 11 valid drying chambers distributed in three sections. The first two sections involved four chambers each, while the remaining section comprised three chambers (D443). Similarly, the result of the superstructure optimization for a 10 m^2 maximum allowable chamber area constraint was five valid drying chambers distributed into two sections The first section involved three chambers, while the remaining two chambers belonged to the second section (D32). For the first case, the total annual cost of the plant was found to be K$84.5/year comprising capital expenses (34.5%) and operational cost (65.8%). For the second case, the total annual cost was less than the first case; roughly K$78.6/year (47.3% capital and 52.7% operational). Percentage of capital cost is increased in the second case, since the drying chambers (comparable in area for both cases) are somewhat more expensive due to the largest area constraint, despite the fact that less sections are required (total area is comparable). Operational cost per chamber is obviously bigger in the second case, but since fewer chambers are involved, the overall performance results in a better design. The performance of the D443 unit results in a total processing expense of 4.6 c/kg wb (reduced to 3 c/kg wb when capital expenses are eliminated). The corresponding value for the D32 is 4.3 c/kg (2.26 c/kg wb based on solely operational performance). This value is almost 10% of the raw material price in the market and, therefore, the drying process cost is only a small portion of the final price of the dehydrated product.

The optimum values for certain operational and construction variables for the produced dryer superstructures of both

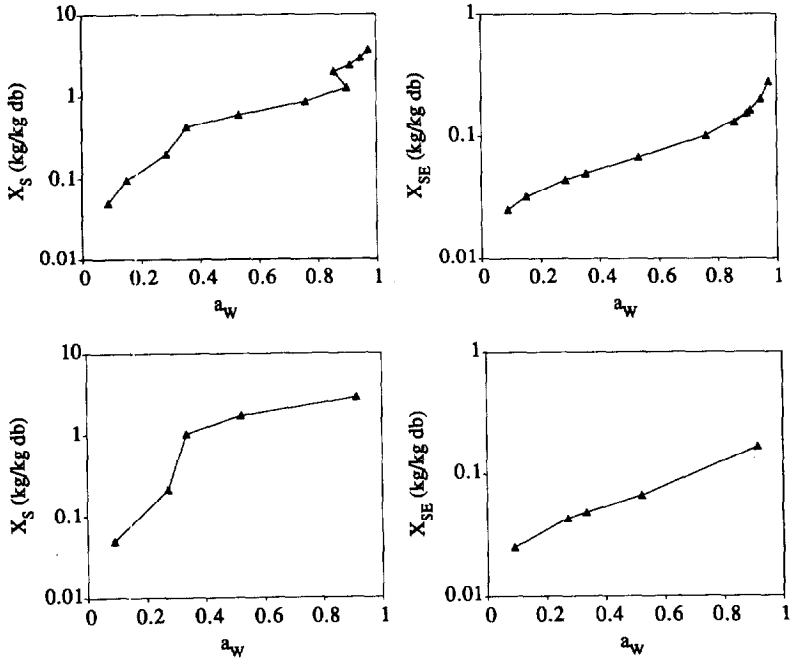

Fig. 2. Actual and equilibrium material moisture content for the optimum structure for both maximum chamber area cases.

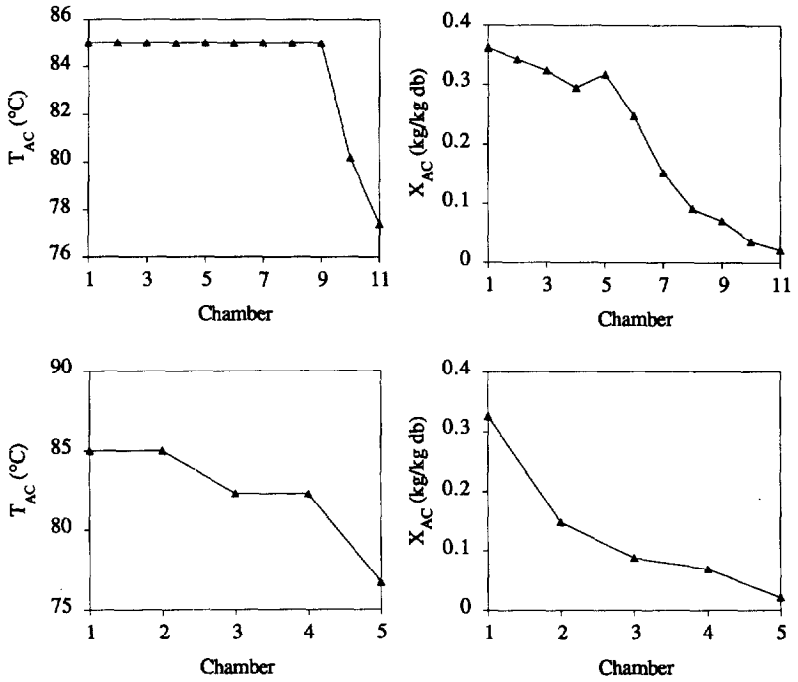

Fig. 3. Temperature and humidity of drying air stream for the optimum structure for both maximum chamber area cases.

cases are included in the diagrams of Figs. 2–7. The optimum chamber area for each dryer was found to be equal to that of the constraint, for both cases. Furthermore, the temperature of the product at the exit of each chamber was found to be uniform for all chambers at the level of the constraint, for both cases. The way that material moisture content potential varied along the optimum structure is shown in Fig. 2. In this Figure, the actual and equilibrium material moisture content at the exit of each of the drying chambers is plotted against air water activity of the rejected air stream. The potential is maintained high, even at the last stages of drying. The general impression is that material moisture content decreases smoothly except for the point where a new section is introduced. Material moisture content decreases considerably at the last stages of drying, at a rate depending on the optimal section configurations and operating conditions involved. The variation of drying air temperature and humidity along sections is illustrated in Fig. 3. In the 11-chamber solution, temperature is kept constant for the first nine chambers to a level constrained by the temperature diminution inequality

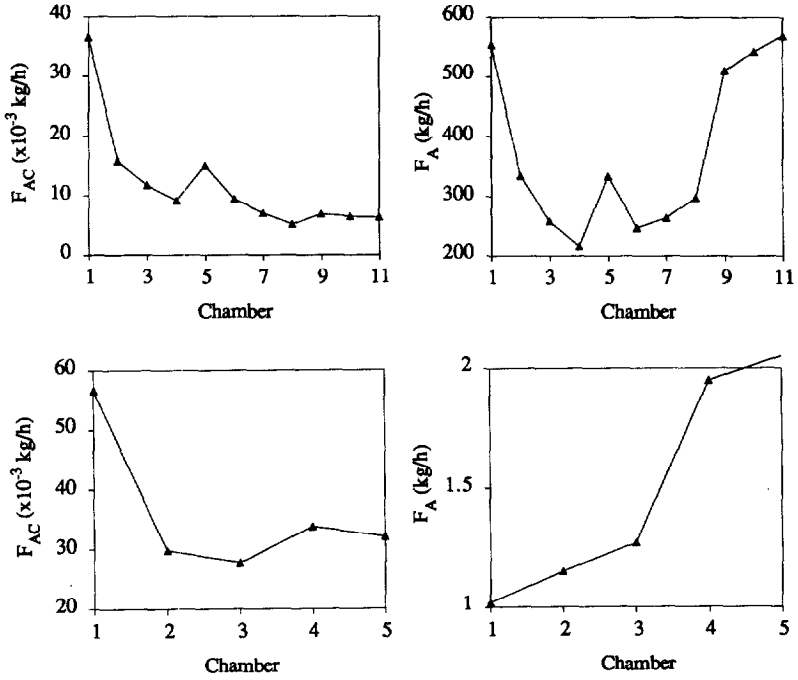

Fig. 4. Air stream flowrates for the optimum structure for both maximum chamber area cases.

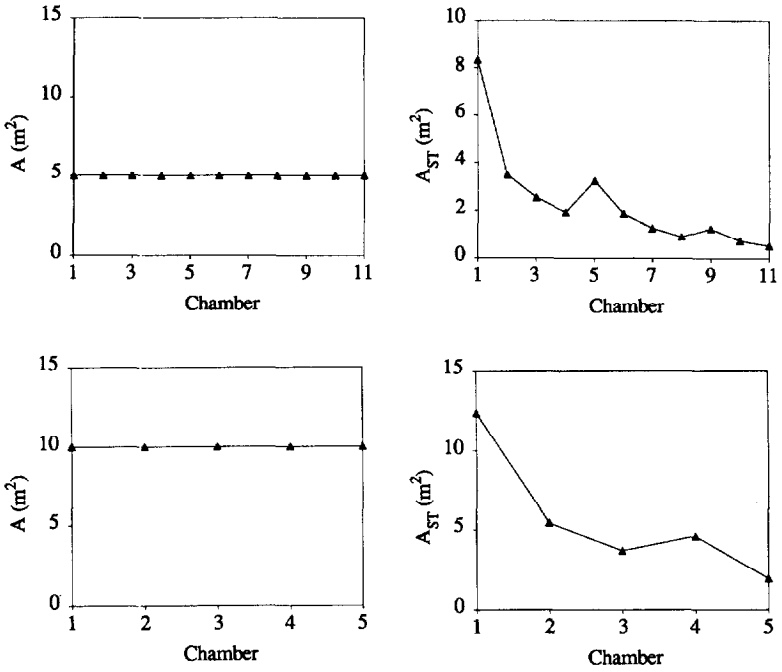

Fig. 5. Chamber and heat exchanger area for the optimum structure for both maximum chamber area cases.

and the demand for maximum product temperature level. Satisfaction of these constraints impose a minimum value for air recirculation in the chamber. At the last two stages of drying however, drying air temperature is forced to decrease, implying higher flowrates for the recirculation of air and increased drying rates, imposing an explicit contribution to capital and operational cost by means of larger fans installed. Drying air humidity decreases smoothly, until a new section is introduced. High humidity values at the first stages of drying are justified by the enormous amount of water vaporized in the corresponding chambers. Fig. 4 shows the way that the air streams flowrate vary at each chamber involved. While the drying air stream flowrate decreases at the last stages of drying, the amount of fresh air needed increases. In this way the appropriate drying potential is maintained. The area of each drying chamber and the corresponding area of heat exchangers used, is given in Fig. 5. Chamber area is the same in all sections, as already stated, while the area of heat exchangers decreases smoothly until a new section is introduced. The huge values of almost all variables in the first chamber of the dryer reveal the dramatic contribution of this stage to the capital and operational cost involved. This is

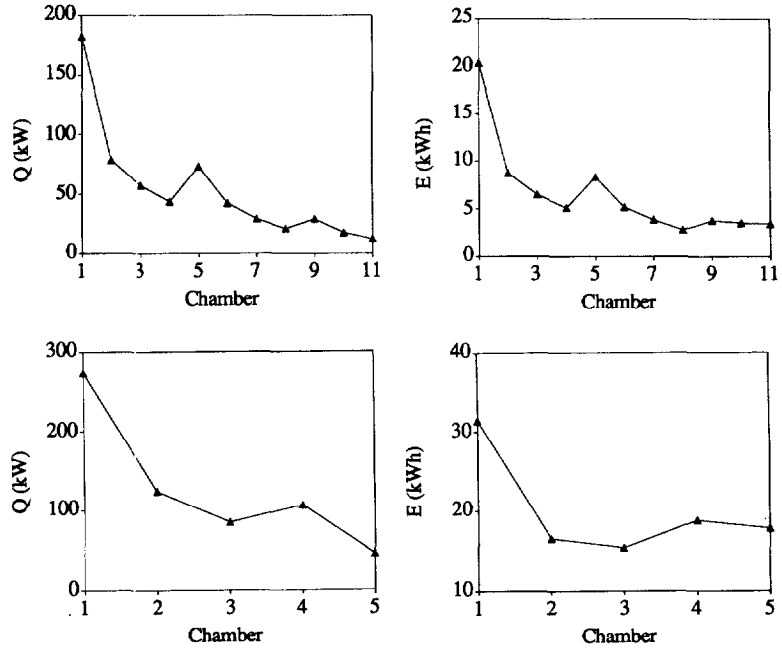

Fig. 6. Heat exchanged and electricity consumed at chamber fans for the optimum structure for both maximum chamber area cases.

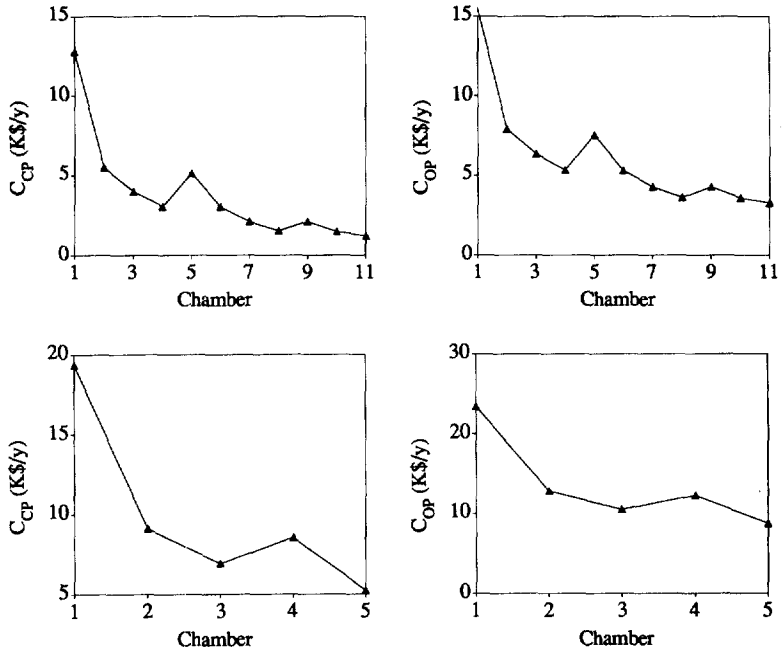

Fig. 7. Total annual cost and its components for the optimum structure for both maximum chamber area cases.

evident also from Fig. 6, which depicts the amount of heat exchanged in chamber heat exchangers and the corresponding consumption of electricity. Section introduction effects are also observed. The total annual cost and its components for each chamber involved are shown in Fig. 7. Evidently, the first chamber consumes the largest amount of energy for water evaporation and product heating and, therefore, its contribution to the total operational cost is important. This also includes capital cost because the need for fans for air recirculation and heat exchangers for air heating are correspondingly high when compared to the rest.

Similar results are obtained by examining the optimum design performance of the second case, five chambers presented in the same Figures. The general impression is that smoothing of curves is interrupted by the introduction of a new section. This is explicable since in each drying section, the velocity of the conveyor-belt, and therefore, its corresponding residence time (1.1, 3.3 and 4.1 h for the three sections of D443, total 8.4 h, and 2.7 and 6.6 h for the two sections of D32, total 9.3 h) changes; this results in completely new drying characteristics within subsequent sections. The total residence time for D32 is almost 1 h greater than for D443. An explicit comparison suggests that despite the economic superiority of D32 over D443, we might select D443 when production demand requires a more rapid dehydration.

In the previous paragraphs, all dryer structures involved, were compared on economic grounds for a specific production capacity of the plant. A detailed analysis of design aspects can substantially aid the selection procedure; if accurate information on construction and operational variables is known, then other criteria can also be taken into consideration to distinguish between similar design results. The total design performance of all configurations can be evaluated if the procedure adopted is carried out for a large number of production capacities. More specifically, if the production capacity (product flowrate) is considered to vary, then the corresponding optimal total annual cost of each dryer can be estimated, its best configuration construction and operational characteristics are evaluated and, therefore, a great number of related flowrate–optimal cost pairs can be obtained for the same process ecumenic parameters (2000 h/year operation and 5 year capital expenses pay-off).

The conveyor-belt dryer case serves as an example. The corresponding flowrate–optimal cost curve for both maximum area values considered is given in Fig. 8. Each point on the corresponding curve results from an optimization procedure similar to the one for the 150 kg/h case. The form of the curves is linear, except only for very low product flowrates. It is evident that if this region is not taken into consideration, the 10 m^2 design is better than the 5 m^2 one. Each curve is distributed into parts where a specified dryer configuration is the best over all other rival structures. Within the production capacity range up to 250 kg/h db, dryer structures from D11 to D666 were evaluated for the 5 m^2 case, while for the 10 m^2 case the evaluated structures involved D2 to D44. The solid points on the curves represent the introduction of a new structure, that is to say the best structure for lower production capacities is substituted by a different structure that exhibits better economic performance for higher product flowrates. If the dryer structure is specified, and all other construction (heat exchangers, fans etc) and operational (temperatures, humidities, etc.) variables are allowed to vary, similar structure-specified flowrate–optimal cost curves can be obtained as those for D11 and D432, presented in Fig. 8. These curves have an exponential form signifying the nonlinear way that optimum cost varies for a given flowsheet configuration. Since these curves have a common point, D432 is worse than

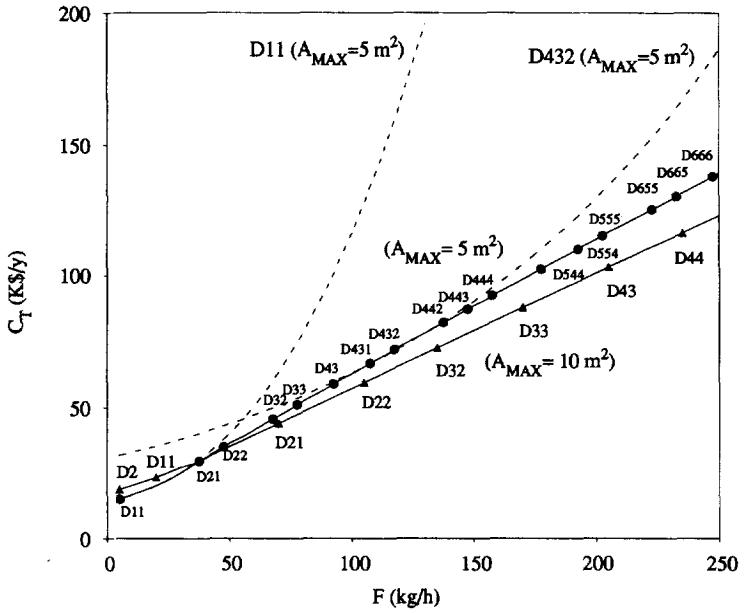

Fig. 8. Optimum total cost versus production capacity for both maximum chamber area conveyor-belt drying structures.

D11 for flowrate values less than roughly 60 kg/h db. For the remaining cases, D11 is very expensive compared to D432. The sections of these curves common to those comprising the overall optimum structures, signify that for the flowrate range corresponding to them, the specified structure is the best compared to its rivals; up to 40 kg/h db for the D11 case and from 130 to 145 kg/h db for the D432 case. Clearly, there are structures not included in the overall optimal cost curve; obviously, these configurations are worse than those participating in the curve. The overall optimum cost curve is the geometrical locus of all such configuration-depended curves. We note a rather regular introduction of new drying chambers to the existing structures as production capacity increases; the number of drying chambers in each section is uniformly increased up to a level until a new section is introduced.

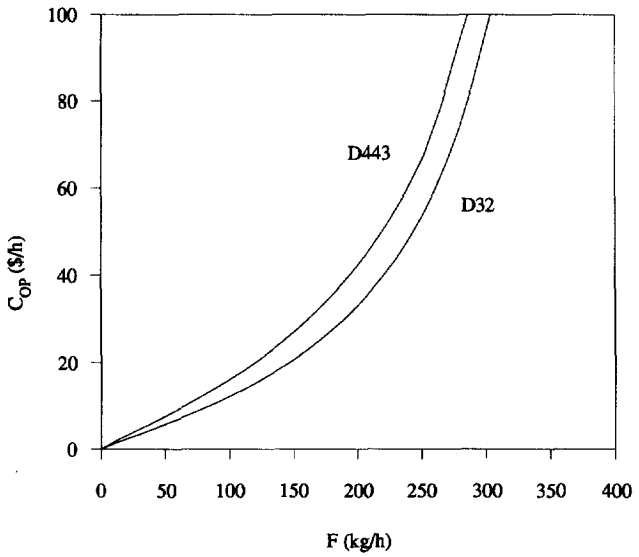

Fig. 9. Optimum operational cost versus production capacity for both maximum chamber area conveyor-belt drying structures.

6. Application to dryer operation

Suppose that a dryer is constructed based on specific demands for the production capacity. It is common experience that the plant is designed so that its dryers can operate to different production schedules based on market demands, and the specified purchased equipment should be able to meet various production constraints and work with different product flowrates. In the case where the flowsheet structure and its corresponding construction characteristics are specified, optimal operational parameter levels can be found by minimizing the dryer operational cost.

For a nominal product flowrate for the dryer operation, then the resulting optimal operation problem can be dealt with by means of the mathematical programming approach mentioned in the previous sections for all dryer configurations involved. Since all construction and structural variables are given, the number of design variables that remain, is substantially reduced and therefore, the resulting NLP problem is significantly simplified. In this case, the optimal operational cost can be expressed as a function of product flowrate, for a given flowsheet configuration. If the production capacity is considered to vary, then the corresponding optimal operational cost can be estimated for a given structure and, therefore, a great number of related flowrate–optimal operational cost pairs can be obtained.

For example, for the 150 kg/h db case in the previous sections, the corresponding flowrate–optimal cost curves are given in Fig. 9. These curves are also considered to be extremely important, since they include concentrated information for the dryers 'operational behaviour'. The shape of the curves exhibit a linear performance for small values of

product flowrate, up to a certain production level, but then the operational cost is greatly increased until the maximum production level is reached. Clearly, the proposed structures are unable to process the specified product when the production level exceeds this extreme value.

Figs. 8 and 9 are the essence of the dryer selection procedure adopted. Design is compared versus operational performance to reach a final decision. Conveyor-belt dryers in the case of food products are probably a very reliable test of the procedure. The results of the analysis adopted are based on strictly economical and technical criteria. Obviously, a different cost scenario would produce completely different results.

7. Conclusion

Dryer selection procedure can be substantially aided by evaluating the design versus performance characteristics. The design aspects can be successfully studied by constructing the optimal total annual cost curves over a production capacity region. These curves contain concentrated information on design with respect to optimum flowsheet structure, sizing and operational parameters. They are evaluated by optimizing the total annual cost of a specific dryer configuration over the entire range of process variables. The process could be adequately described by a simple mathematical model. When a design configuration is implemented, its operational performance can be investigated by suitably constructing optimal operational cost curves over a wide product flowrate range. These curves reveal the performance under various product demand scenarios imposed by the market.

This methodology was applied to the case of continuous conveyor-belt dryers. This type of dryer produces satisfactory results with respect to design and operation. The methodology has been successfully applied to the drying of sliced potato.

8. Nomenclature

A	Area of cross section of dryer (m^2)
A_1, A_2, A_3	Constants of Antoine Eq. (34)
A_{MAX}	Maximum constructed area for each drying chamber (m^2)
A_{ST}	Area of heat exchanger (m^2)
a_W	Water activity of air stream leaving the product section
a_{WC}	Water activity of air stream entering the product section
C_{CP}	Capital annual cost ($/year)
C_E	Cost of electricity unit ($/kWh)
C_{OP}	Operational annual cost ($/year)
C_{PA}	Specific heat of air (kJ/kgK)
C_{PS}	Specific heat of dry solid (kJ/kgK)
C_{PV}	Specific heat of vapor (kJ/kgK)
C_{PW}	Specific heat of water (kJ/kgK)
C_{ST}	Cost of steam unit ($/kg)
C_T	Total annual cost ($/year)
d_P	Particle diameter (m)
e	Percentage of capital cost on annual rate
E	Electrical power consumed for the operation of fans (kWh)
F_A	Flowrate of fresh air stream (kg/h db)
F_{AC}	Flowrate of drying air stream (kg/h db)
F_S	Flowrate of product stream (kg/h db)
F_{ST}	Flowrate of steam (kg/h)
h_A	Specific enthalpy of wet air stream (kJ/kg)
h_S	Specific enthalpy of humid product (kJ/kg)
k_M	Drying constant (1/h)
$k_0, k_1, k_2, k_3, k_4, k_5$	Constants of drying constant Eq. (33)
m	Drying section of a conveyor-belt dryer
$m_{W,A}$	Molecular weight of air (kg/kmol)
M	Number of drying sections of a conveyor-belt dryer
n	Drying chamber of a conveyor-belt dryer
n_{SC}, n_D, n_F, n_{ST}	Constants of capital cost function
n_m	Number of drying chambers of drying section m
N	Number of drying chambers per section of conveyor-belt dryer
P	Total pressure (kPa)
P^{sat}	Water vapor pressure (kPa)
Q	Exchanged heat rate (kW)
t	Residence time (h)
t_{OP}	Operating time for dryer operation (h/year)
T_A	Temperature of output air stream (°C)
T_{AC}	Temperature of drying air stream (°C)
T_{AM}	Temperature of mixed recirculation and fresh air streams (°C)
T_{AO}	Temperature of fresh air stream (°C)
T_{S-}	Temperature of product stream on entering the chamber (°C)
T_{S+}	Temperature of product stream on leaving the chamber (°C)
T_{SF}	Desired value of material temperature leaving the dryer (°C)
T_{ST}	Temperature of steam (°C)
$T_{S,MAX}$	Maximum temperature level for no thermal degradation observed (°C)
U_{ST}	Overall heat transfer coefficient at heat exchangers (kW/m^2K)
V_A	Air velocity through product (m/s)
X_A	Absolute humidity of output air stream (kg/kg db)
X_{AC}	Absolute humidity of drying air stream (kg/kg db)

X_{AO}	Absolute humidity of fresh air stream (kg/kg db)
X_{SO}	Nominal value of material moisture content entering the dryer (kg/kg db)
X_{SE}	Equilibrium material moisture content (kg/kg db)
X_{SF}	Desired value of material moisture content leaving the dryer (kg/kg db)
X_{S-}	Moisture content of product stream on entering a drying chamber (kg/kg db)
X_{S+}	Moisture content of product stream on leaving a drying chamber (kg/kg db)
X_M, C, K, C_0, K_0, ΔH_C, ΔH_K	Constants of the GAB Eqs. (30)–(32)

Greek Letters

α_0, α_1, α_2, α_3	Constants of Eq. (37)
α_{SC}, α_D, α_F, α_{ST}	Constants of capital cost function
ΔH_{vap}	Latent heat of vaporization of water (kJ/kg)
ΔH_0	Latent heat of vaporization of water at reference temperature (kJ/kg)
ΔP	Pressure drop of air stream (kPa)
ΔT	Temperature diminution of air stream on passing through the product (°C)
ΔT_{MAX}	Maximum allowed temperature diminution (°C)
λ_B	Mass ratio of water and air molecules
ϱ_A	Density of air (kg/m^3)
ϱ_B	Belt load (kg/m^2 wb)
ϱ_{B0}	Nominal value of belt load at the entrance of each drying section (kg/m^2 wb)

References

[1] C.T. Kiranoudis, Z.B. Maroulis, D. Marinos-Kouris, Int. J. Heat Mass Transfer 38 (1995) 463–480.
[2] Y.K. Ahn, H.C. Chen, L.T. Fan, G.G. Wan, Can. J. Chem. Eng. 42 (1964) 117–120.
[3] T.L. Thompson, PhD Thesis, Purdue University, West Lafayette (1967).
[4] D.M. Farmer, PhD Thesis, Michigan State University, East Lansing, MI (1972).
[5] J.R. Thygeson, E.D. Grossmann, AIChE J. 16 (1970) 749–755.
[6] R.C. Brook, F.W. Bakker-Arkema, J. Food Proc. Eng. 2 (1978) 119–211.
[7] H.A. Becker, P.L. Douglas, S. Ilias, Can. J. Chem. Eng. 62 (1984) 738–745.
[8] R. Bertin, M. Blazquez, Drying Technol. 4 (1986) 45–66.
[9] W. Kaminski, I. Zbicinski, S. Grabowski, C. Strumillo, Drying Technol. 7 (1989) 1–16.
[10] H. Chen, PhD Thesis, University of California, Davis, CA (1990).
[11] G.K. Vagenas, D. Marinos-Kouris, Drying Technol. 9 (1991) 439–461.
[12] C.T. Kiranoudis, Z.B. Maroulis, D. Marinos-Kouris, J. Food Eng. 23 (1994) 375–396.
[13] C.T. Kiranoudis, Z.B. Maroulis, D. Marinos-Kouris, Appl. Math. Modelling 18 (1994) 58–71.
[14] C.T. Kiranoudis, Z.B. Maroulis, D. Marinos-Kouris, Drying Technol. 11 (1993) 1271–1292.
[15] C.T. Kiranoudis, Z.B. Maroulis, D. Marinos-Kouris, Comp. Chem. Eng. 19 (1995) 581–606.
[16] C.T. Kiranoudis, E. Tsami, Z.B. Maroulis, D. Marinos-Kouris, J. Food Eng. 20 (1992) 55–74.
[17] L.K.E. Achenie, L.T. Biegler, Comput. Chem. Eng. 14 (1990) 23–40.
[18] Z. Pakowski, Z. Bartczak, C. Strumillo, S. Stenstrom, Drying Technol. 9 (1991) 753–773.
[19] C.T. Kiranoudis, Z.B. Maroulis, D. Marinos-Kouris, Drying Technol. 10 (1992) 1097–1106.